Recent Progress of Researches in Mirror Devices

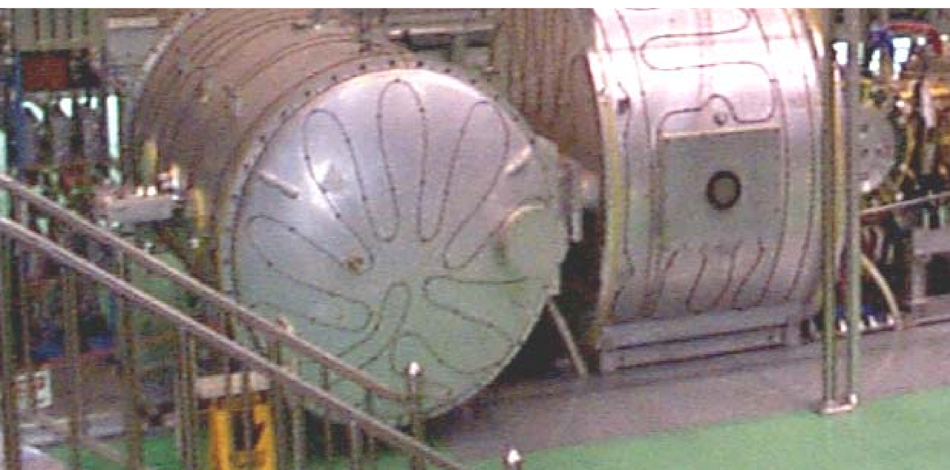

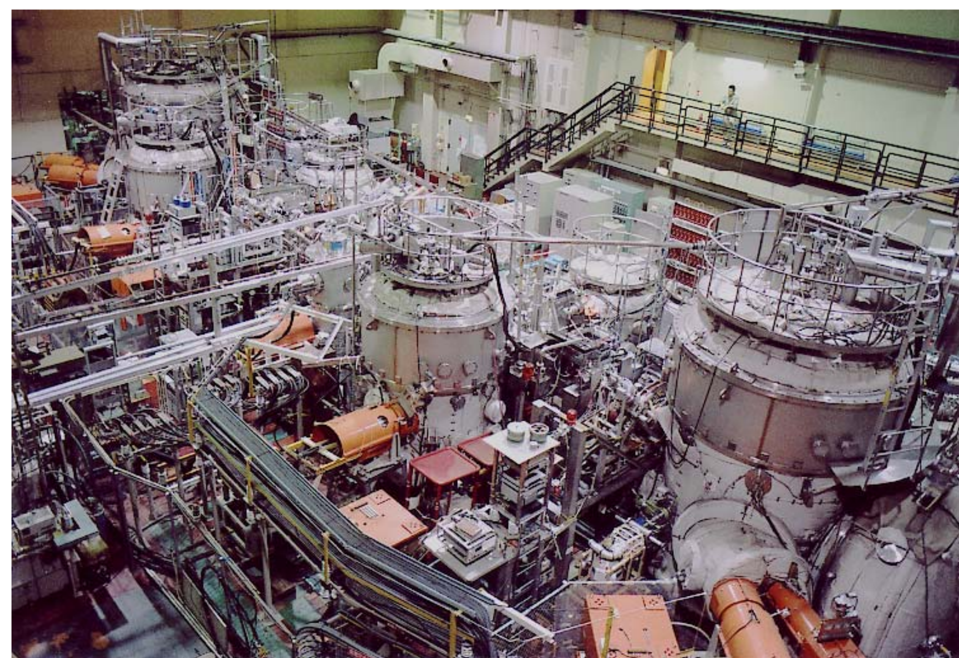

IAEA FEC 2004
November 1 ~ 6, 2004
Vilamoura , Portugal

Heating and Confinement of Ions at Multimirror Trap GOL-3

V.S. Koidan, A.V. Arzhannikov, V.T. Astrelin, A.V. Burdakov, G.E. Derevyankin, I.A. Ivanov, M.V. Ivantsivsky, S.A. Kuznetsov, K.I. Mekler, S.V. Polosatkin,V.V. Postupaev, A.F. Rovenskikh, S.L. Sinitsky, Yu.S. Sulyaev, A.A. Shoshin, Eh.R. Zubairov

Budker Institute of Nuclear Physics, Novosibirsk 630090, Russia

GOL-3

GOL-3 facility

GOL-3

Introduction

Recently magnetic system of the GOL-3 facility was converted into completely multimirror one.

Multimirror plasma confinement

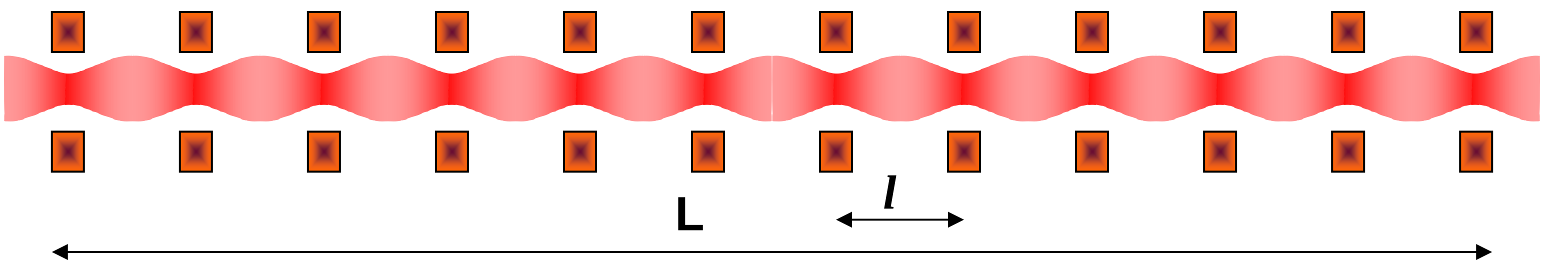

Full solenoid length L exceeds mean free path of the particles λ_i. If, at the same time, the mirror cell length $l < \lambda_i$ then the longitudinal confinement time increases essentially compared to classical single mirror trap.

$$\tau \sim R^2 \frac{L^2}{\lambda_i V_{T_i}} = R^2 \frac{L}{\lambda_i} \tau_0$$

$$R = \frac{B_{max}}{B_{min}}$$

$$\tau_0 \sim \frac{L}{V_{T_i}}$$ -confinement time in solenoid

GOL-3

GOL-3 facility

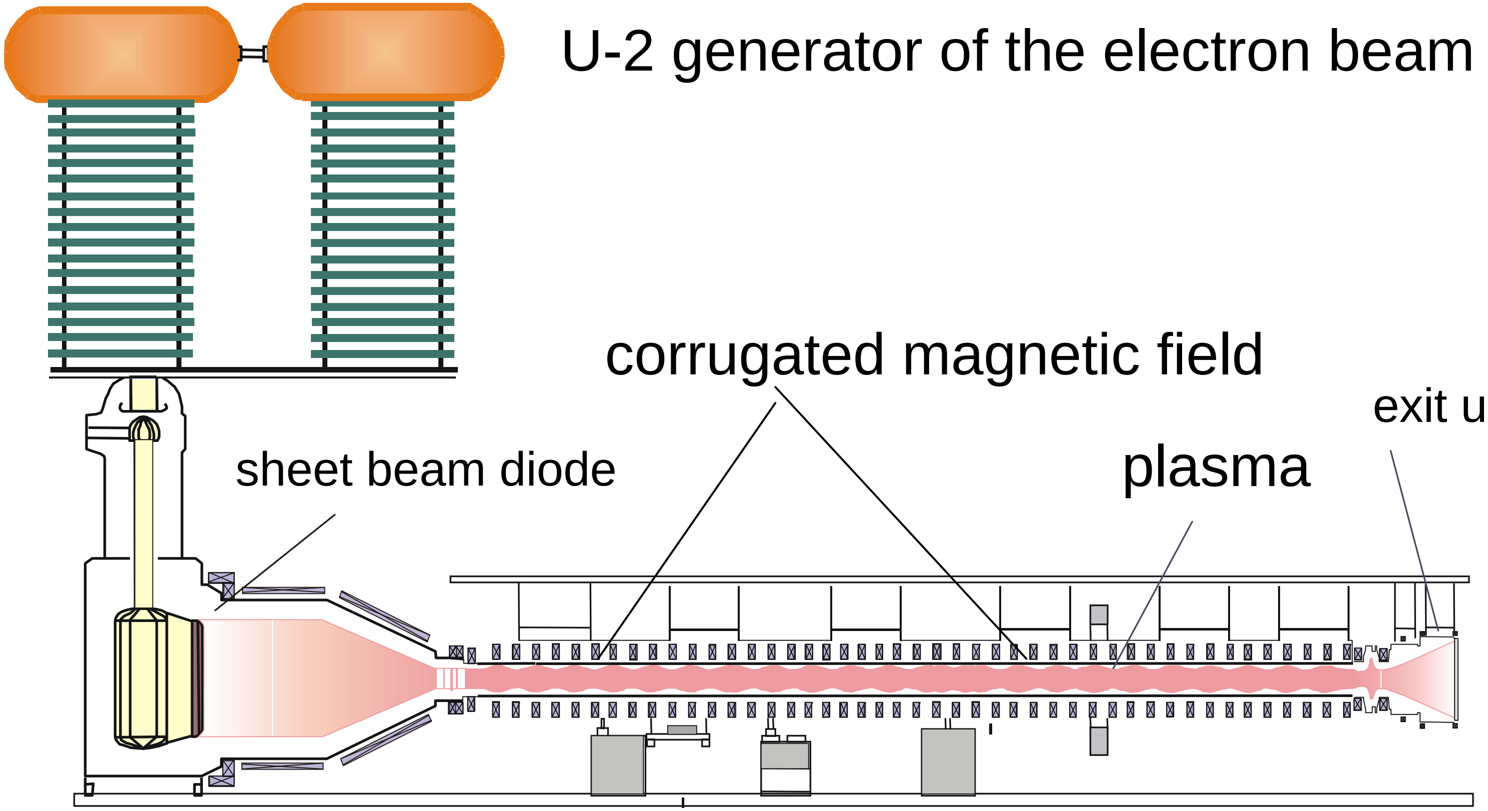

Magnetic field
- multimirror
- 55 cells
- 4.8/3.2 T

Plasma

Length ~ 12 m

Density - 10^{20} - 10^{22} m^{-3}

Temperature ~ 1 keV

Electron beam

Energy	- 1 MeV
Current	- 50 kA
Energy content	- 0.3 MJ
Pulse duration	- 8 μs

GOL-3

Plasma heating and confinement

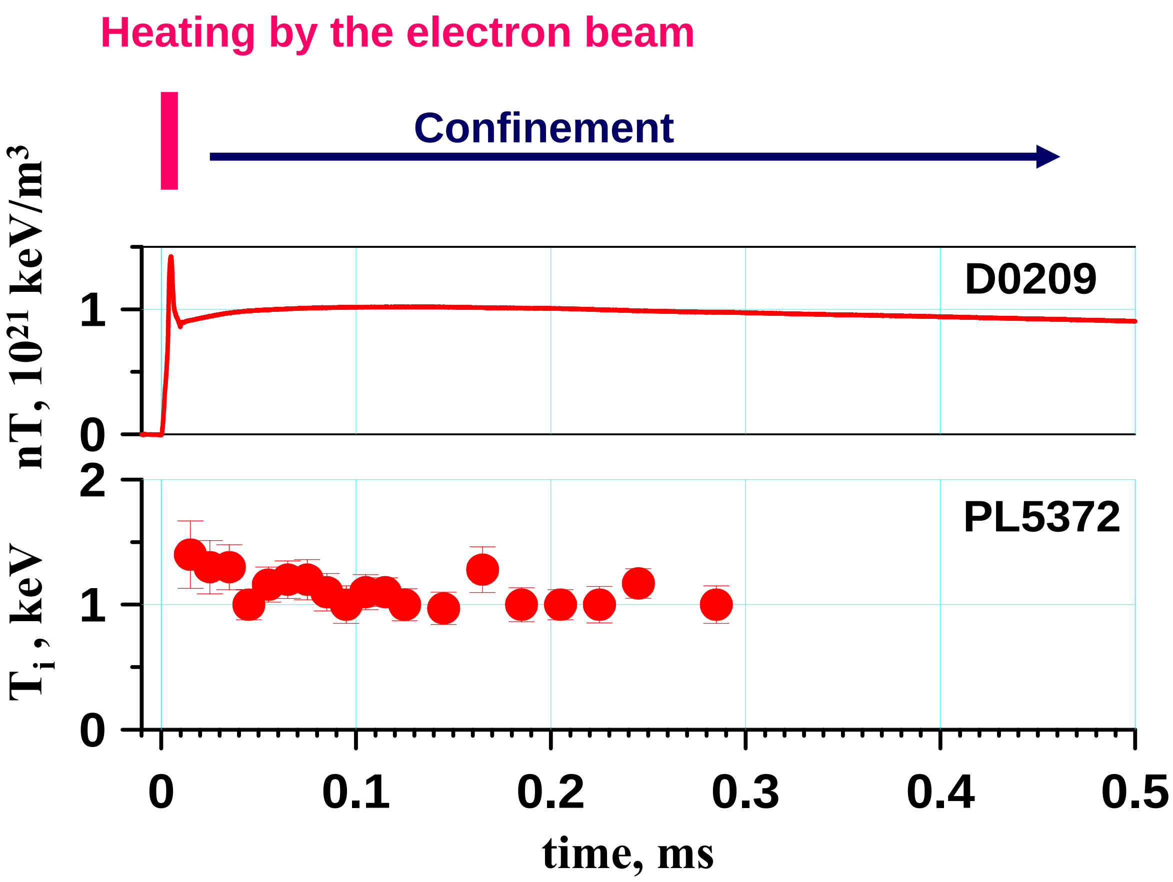

Dynamics of ion temperature measured by Doppler broadening of D_α spectral line . Initial density is $0.5 \cdot 10^{21}$ m^{-3}.

- Collective plasma heating by E- beam results in T_e~2 keV at ~$0.5 \cdot 10^{21}$ m^{-3} density. High T_e exists for ~10 μs.
- To this time T_i reaches 1-2 keV and keeps at the high level long enough time.
- Duration of the ion heating is much less than classical electron-ion energy transfere time.
- In order to explain this phenomenon the mechanism of fast ion heating is suggested.

GOL-3

Neutron generation

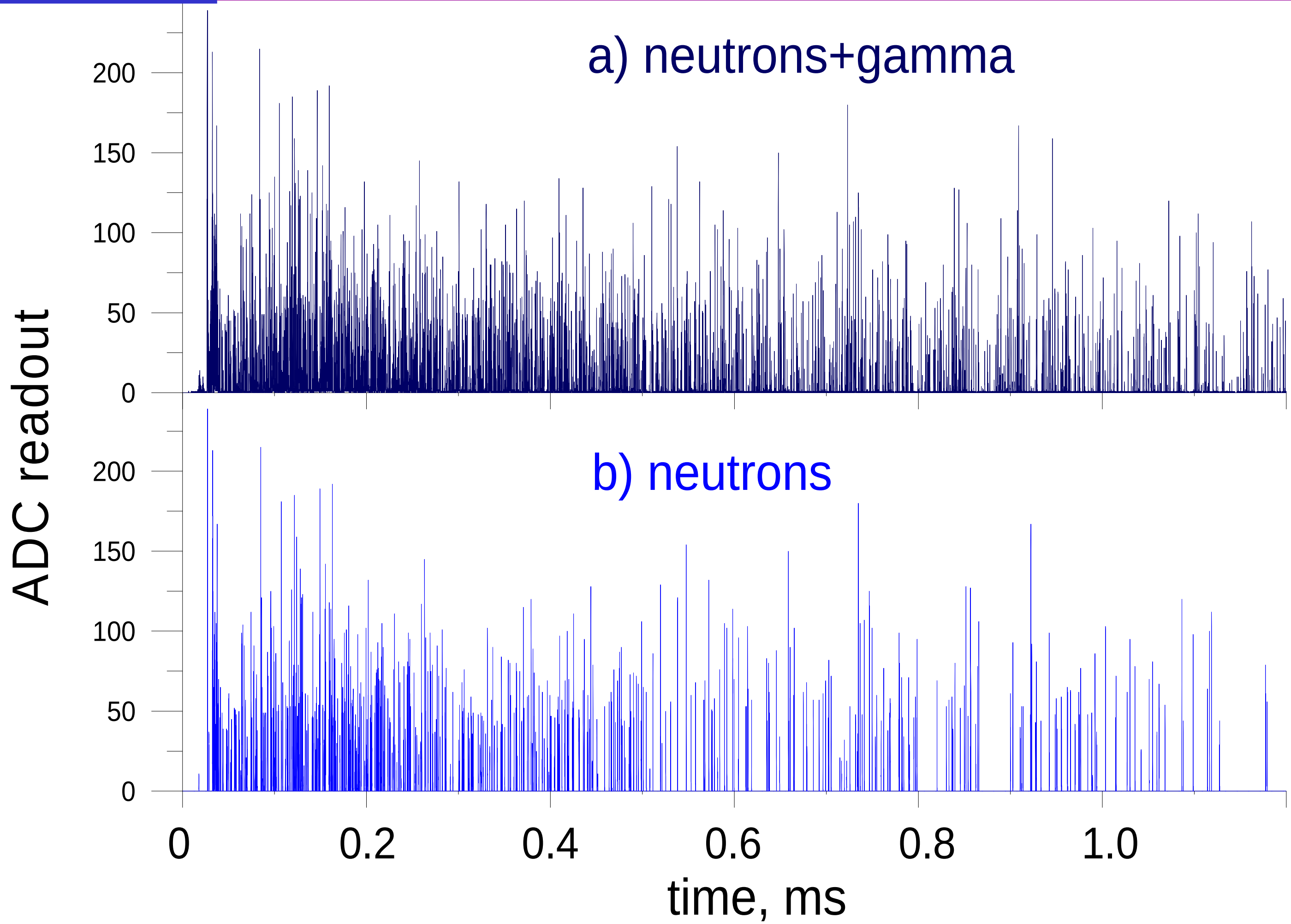

Waveforms of signal of digital PSD stilbene detector (Z=4.3 m).

a) original signal, which contain neutron and gamma components of fusion product emission. Digital pulse shape discrimination (dPSD) was used for analysis of stilbene detector signals.

b) signal of fusion neutrons (after separation by dPSD). Initial density is $1.9 \cdot 10^{21}$ m^{-3}.

GOL-3

Progress in GOL-3 parameters

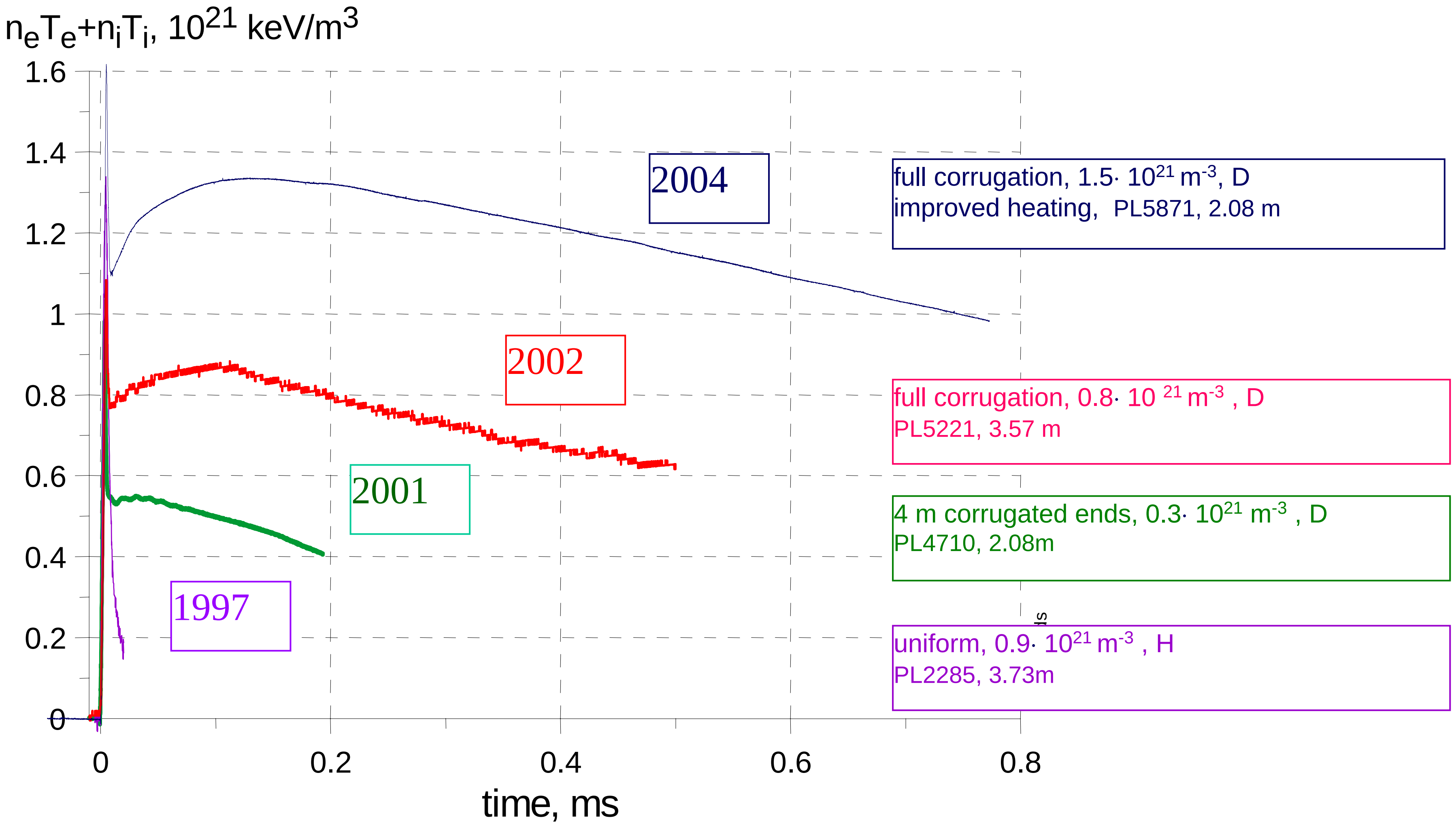

Waveforms of the plasma pressure in the GOL-3 facility at different magnetic configurations

GOL-3

Results

- ***Conditions for stable creation and effective heating of plasma in the range*** $(0.2 \div 6) \cdot 10^{21}$ ***m***$^{-3}$ ***are experimentally found.***

- ***Electron and ion plasma temperatures up to 2 keV at density*** $\sim 10^{21}$ ***m***$^{-3}$ ***are achieved.***

- ***Macroscopical stability and long confinement of the dense plasma in multimirror system is obtained.***

- ***The value*** $n\tau_E \sim (1.5 \div 3) \cdot 10^{18}$ ***m***$^{-3}$***s at ion temperature ~1 keV is attained.***

Advances in Potential Formation and Findings in Sheared Radial Electric-Field Effects on Turbulence and Loss Suppression in GAMMA 10

T. Cho, H. Higaki, M. Hirata, H. Hojo, M. Ichimura, K. Ishii, M. K. Islam, A. Itakura, I. Katanuma, J. Kohagura, Y. Nakashima, T. Numakura, T. Saito, Y. Tatematsu, M. Yoshikawa, M. Yoshida, T. Imai, V. P. Pastukhov*, and S. Miyoshi

Plasma Research Centre, University of Tsukuba, Japan

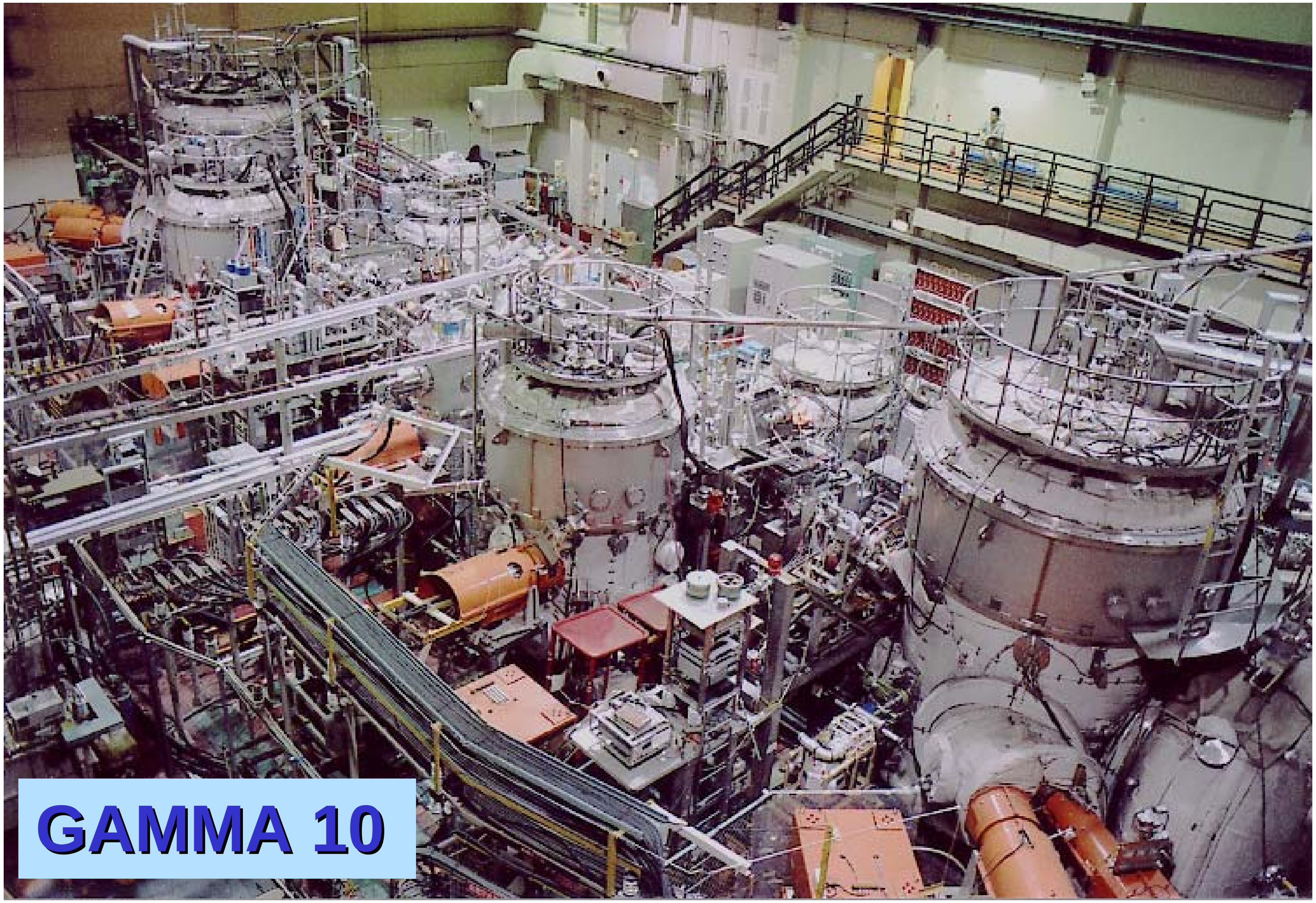

Three-Times Progress in *Ion-Confining Potential* ϕ_c

After IAEA 2002 (Lyon)

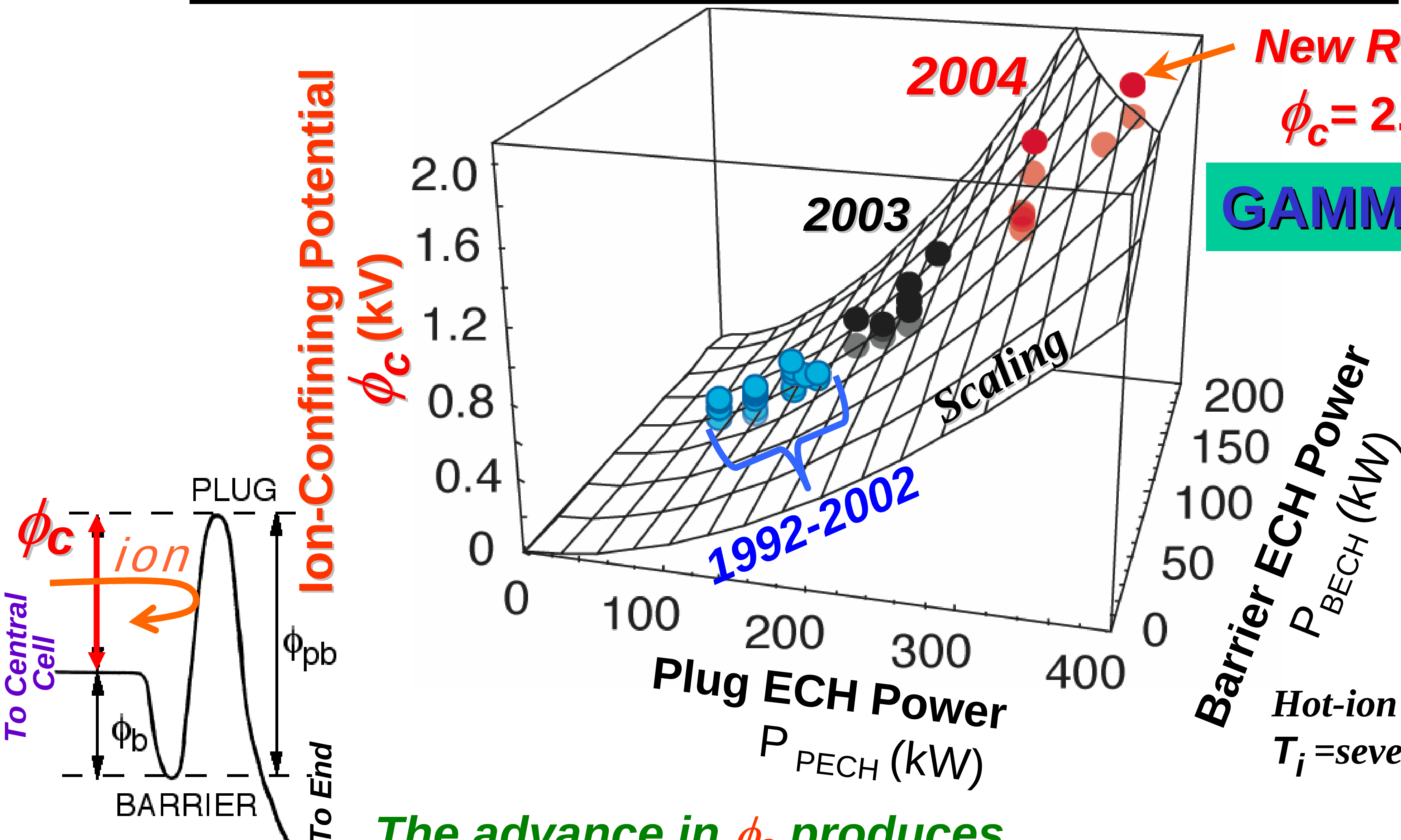

Hot-ion mode
T_i =several keV

The advance in ϕ_c produces strong radially sheared electric fields E_r.

Suppression of Drift Waves and Turbulent Fluctuations by Radially Sheared Electric Fields E_r

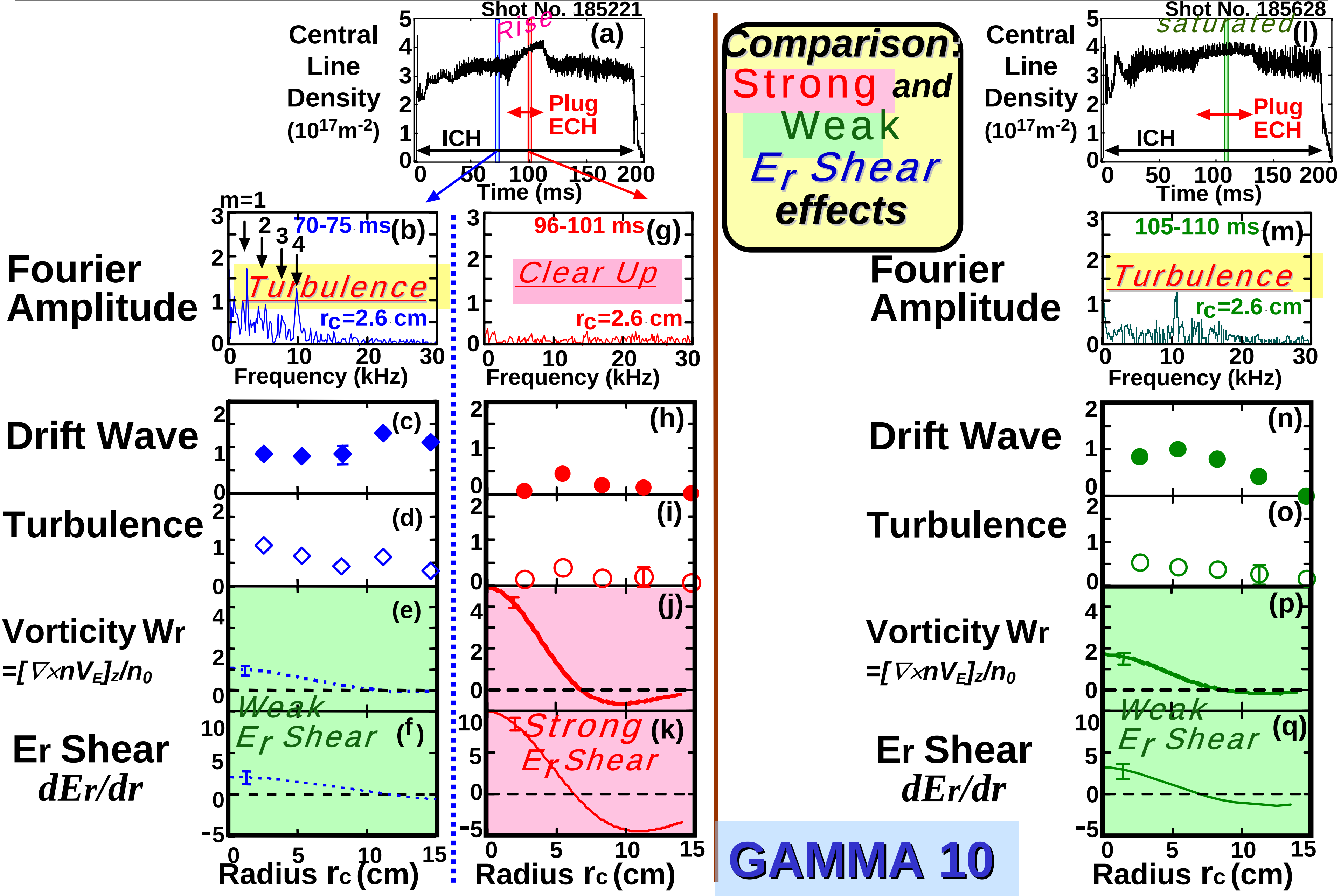

Observations of Turbulent Vortex Structures, and their Suppression due to a strong E_r Shear formed by High-Potential production.

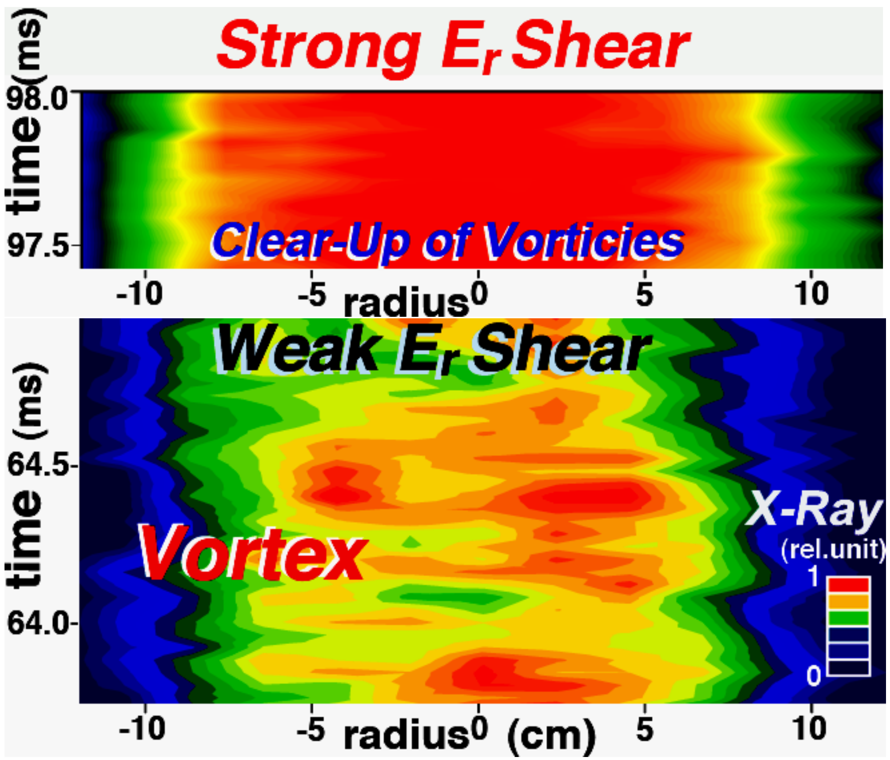

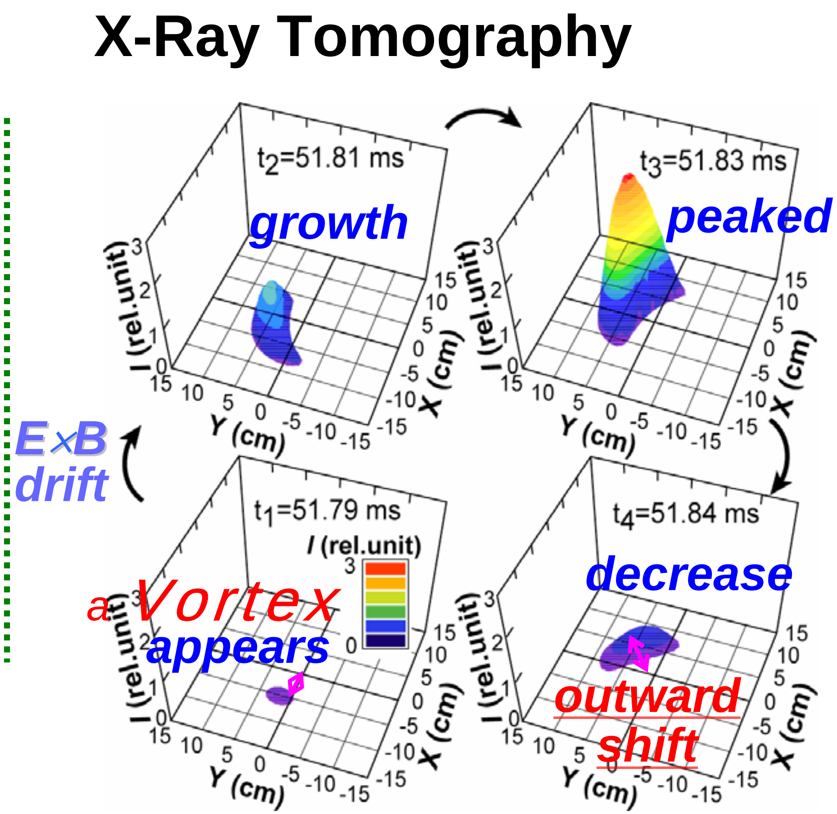

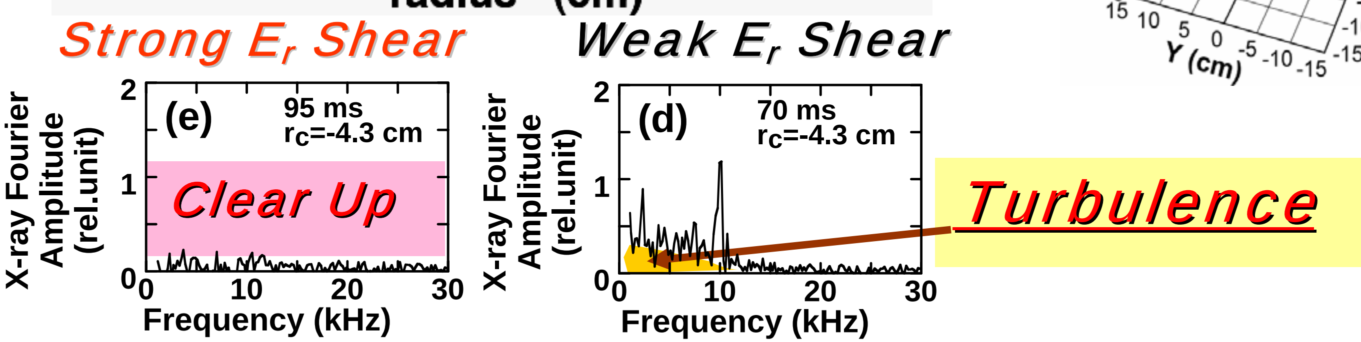

GAMMA 10

Confinement Improvement by Turbulent Vortex Suppression due to a Strong E_r Shear

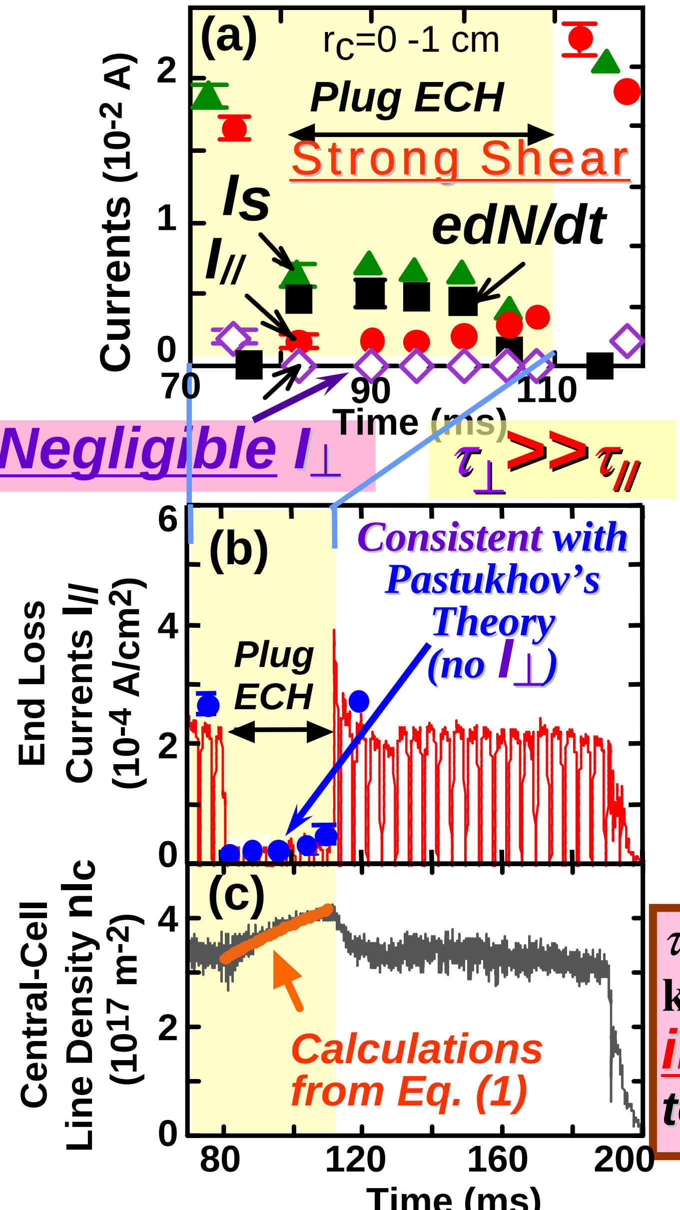

Particle Balance Equation (1);

$$e\frac{dN}{dt} = I_s - I_{//} - I_{\perp}$$

■ ▲ ● ◇

dN/dt ; density rise

I_s ; source current (Hα data)

$I_{//}$; endloss current

$I_{\perp}$; transverse-loss current *from Eq.(1).*

(Nonambipolar loss is suppressed with floated endplates.)

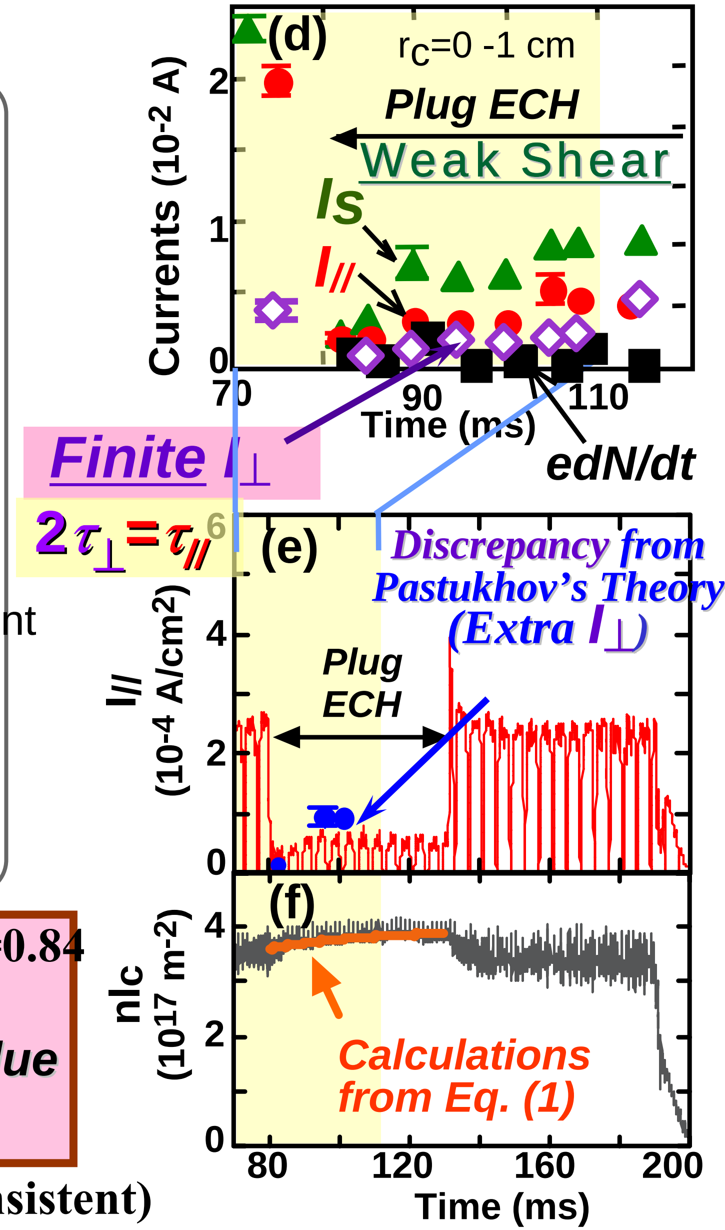

$\tau_{p//}$=95 ms, $\tau_{\perp}$>4 $\tau_{//}$ for ϕ_c=0.84 kV; *a few tens % improvement in $\tau_{\perp}$ due to a strong shear*

($\tau_{E\text{-Pastukhov}}$=50 ms; consistent)

Scalings for *High Potential* and the associated *Strong E_r Shear Formation*

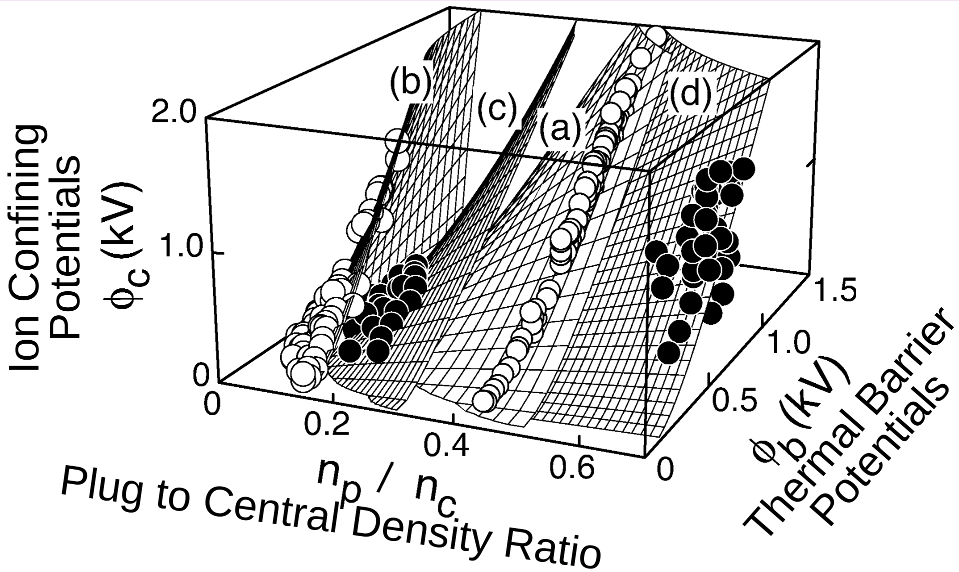

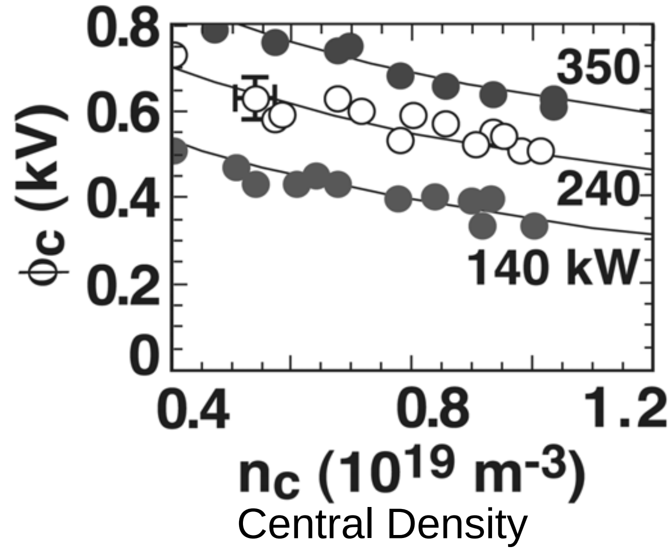

Validity of our proposed theoretical surfaces *for potential formation* [1]

covering various modes including

(a) high-potential and (b) hot-ion modes.

Data well fit to the extended scaling surfaces *with auxiliary heatings*; *i.e.,*

(c) and (d) with central ECH

(d) along with plug NBI.

[1] T. Cho *et al.*, Phys. Rev. Lett. 86, 4310 (2001).

A preferable scaling of ***a weak decrease in ϕ_c with increasing n_c***

together with the ***recovery of ϕ_c with increasing ECH powers***

(a hot-ion mode having T_i>keV)

GAMMA 10

Summary in GAMMA 10

[1] Three-times Progress *in Ion-Confining Potentials* ϕ_c as compared to ϕ_c in 1992-2002 ***is achieved*** in the hot-ion mode.

[2] **The** advance **in the potential formation** ***leads to*** a ***finding*** of ***remarkable effects of radially produced*** E_r *Shear*, dE_r/dr.

[3] *Turbulent Vortex structures* ***are observed*** with a **weak** E_r **shear** formation.

[4] *Suspression* ***of the turbulent vortex structures*** **due to a strong** E_r **shear** ***leads to*** *Confinement Improvement in the* ***transverse direction*** (typically a few tens %).

[5] **The** *progress* **in the** *potential formation* is made ***in line with the*** *extension* **of** *our proposed physics scaling*.

[6] A scaling **of** ϕ_c with n_c (ranging in achieved n_c~10^{19} m^{-3} with T_i ~ keV for ϕ_c >hundreds V) is found to have **preferable dependence** of **a** weak decrease **in** ϕ_c **with increasing** n_c along with **the** recovery **of** ϕ_c **with increasing ECH powers**.

HANBIT Mirror Device and Recent Research Activities

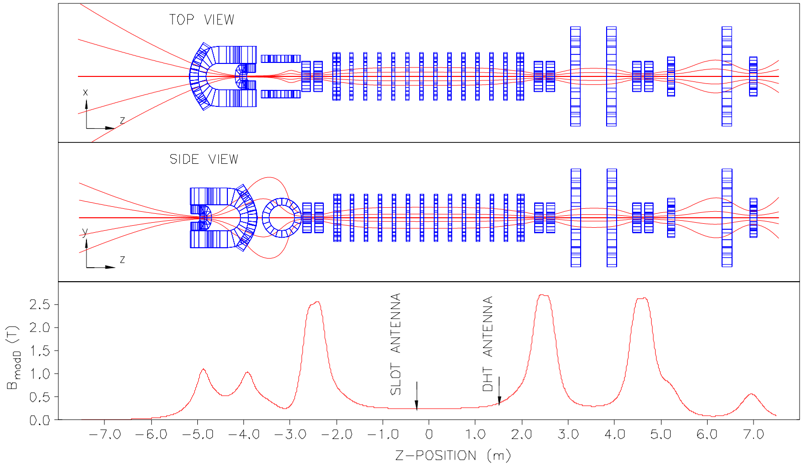

Major Recent Research Activities (after Lyon Conference) :

- Identification of discharge characteristics in HANBIT
- Development of stable reference operation scenarios in HANBIT
- Basic physics study of plasma heating, stability, and confinement
- Hot electron-ring experiments in plug region, KS in cusp region.
- ECH preionization or heating experiments in central cell

Two distinct operation regimes observed in HANBIT

(IAEA2002, Lyon)

- Big density jump observed near $\omega \sim \omega_{ci}$ during initial HANBIT experiments

(the density jump point is $B_{cc} \sim 107\%$ or ~ 0.23 T, where $\omega_{ci} \sim \omega$ (f= $\omega/2\pi$=3.5MHz)

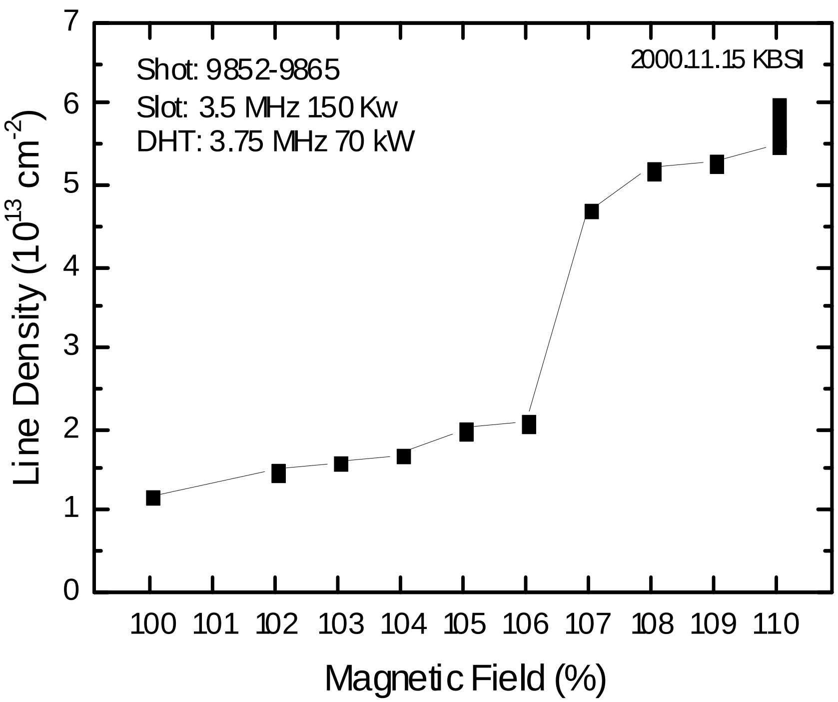

- Measurements show also the jump in plasma beta and ion temperature

- A possible scenario of the improvement

  - Slow wave ion heating at $\omega < \omega_{ci}$ => T_i , T_i / T_e increase => confinement improvement => density, beta increase

  - Hot ions => fast neutrals by charge exchange => increased wall-recycling => self-sustainment of discharge without fueling

** MHD mode stabilization by RF ponderomotive or side-band coupling may be also a possible trigger.

Studies on Stability

- Power excursion experiments were done to find ***threshold power*** below which the plasma discharge is terminated.
- Power excursion experiments reproduced the characteristics of **operation window** found in normal operation.

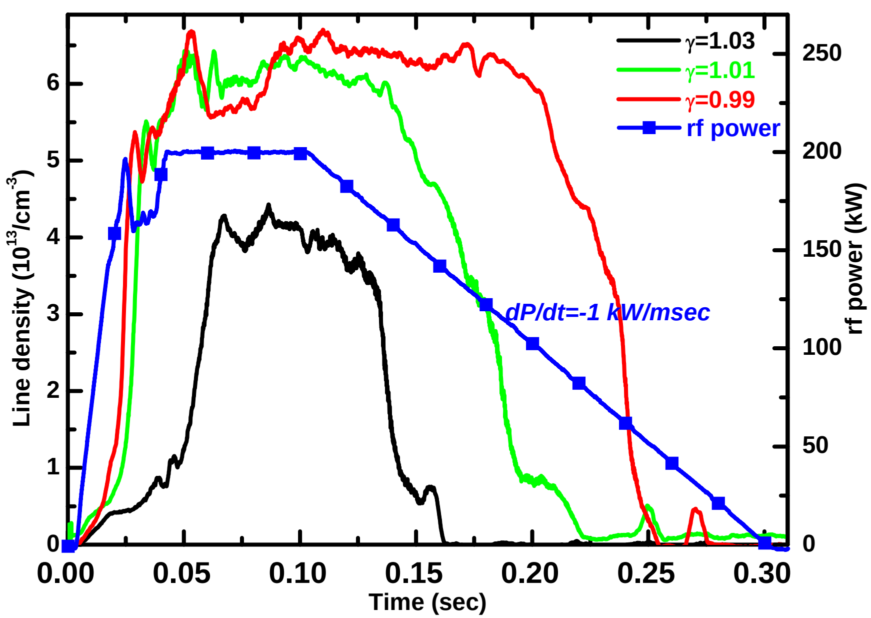

- FFT of edge probe data for different time periods shows the **onset of a strong MHD activity (~ 3 kHz)** before/during the plasma termination.

- Array probe data show ***m=-1*** ***(ion diamagnetic direction),*** ***n=0 interchange*** mode is excited.

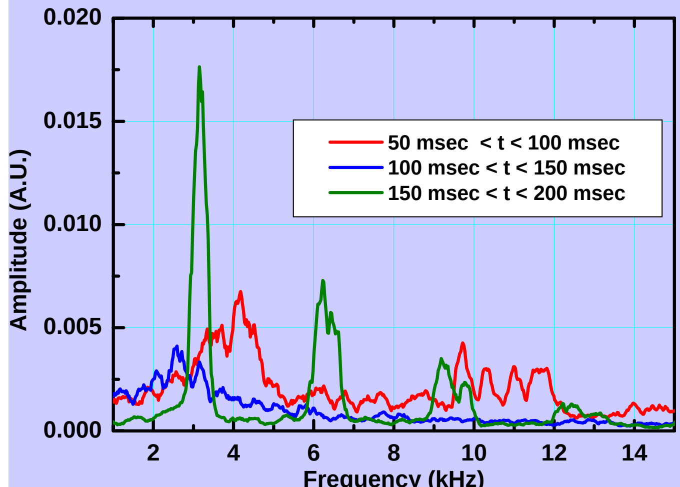

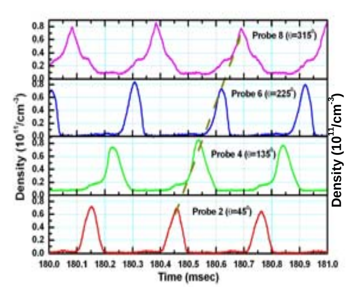

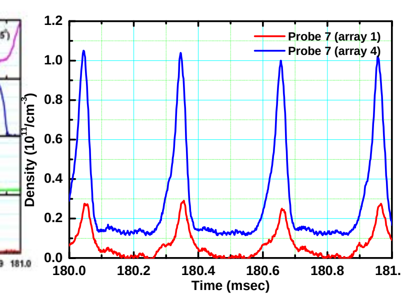

Wavelet Transformation

- The instability onset time of both probes are the same about 82 ms and finishes at 137 ms.
- Plasma column movement in the radial direction is not observed.
- A fundamental 3.3 kHz and its second harmonics are shown in both probes.
- Wavelet power spectrum of the edge probe is much smaller than that of the inner one.

- About 3.5 MHz frequency is dominant.
- Wavelet power spectrum during interchange mode is much weaker than that of the quiescent plasma.
  - RF power was reduced by factor of 2
  - wave coupling effects are efficient during interchange instability

Edge probe at r = 160 mm

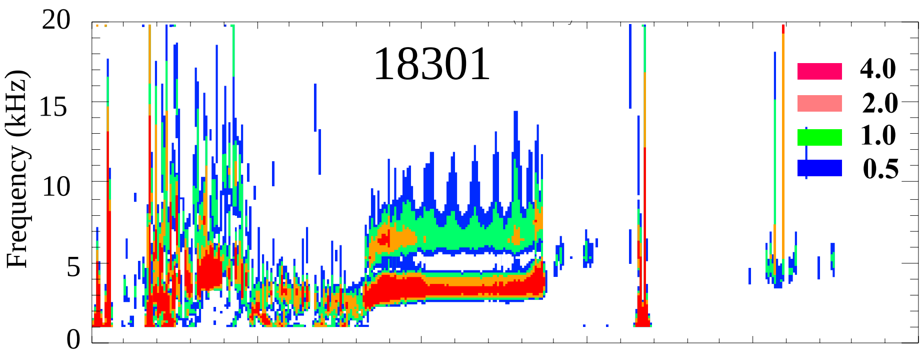

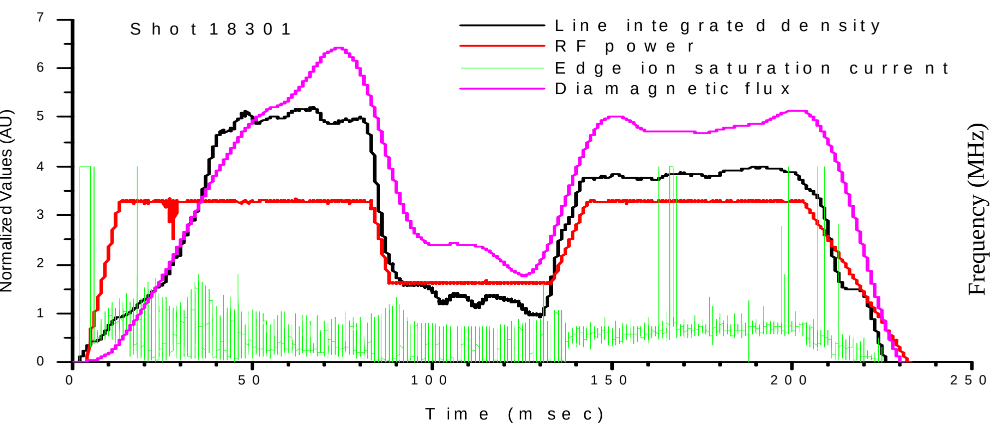

Magnetic probe at r = 160 mm

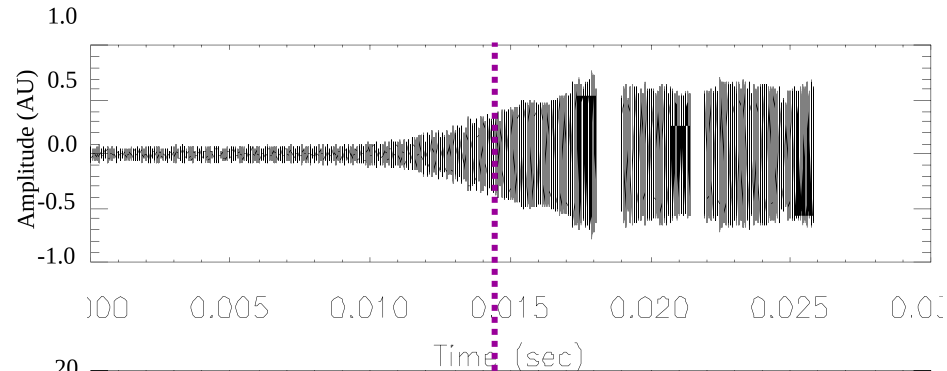

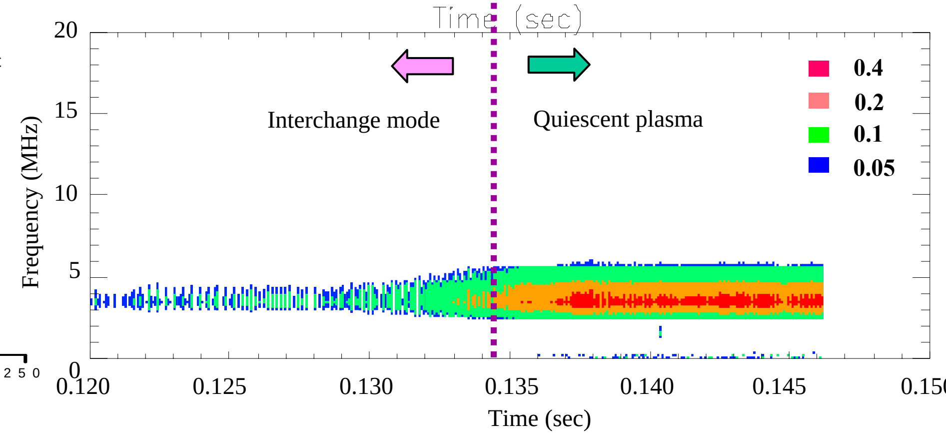

Ponderomotive Theory

- Full wave simulation taking into account the **density profile** and realistic **mirror field geometry** showed that ponderomotive force **destabilizes** interchange modes when **γ=0.97 and stabilizes** when **γ=1.03** → **disagree with experiments**

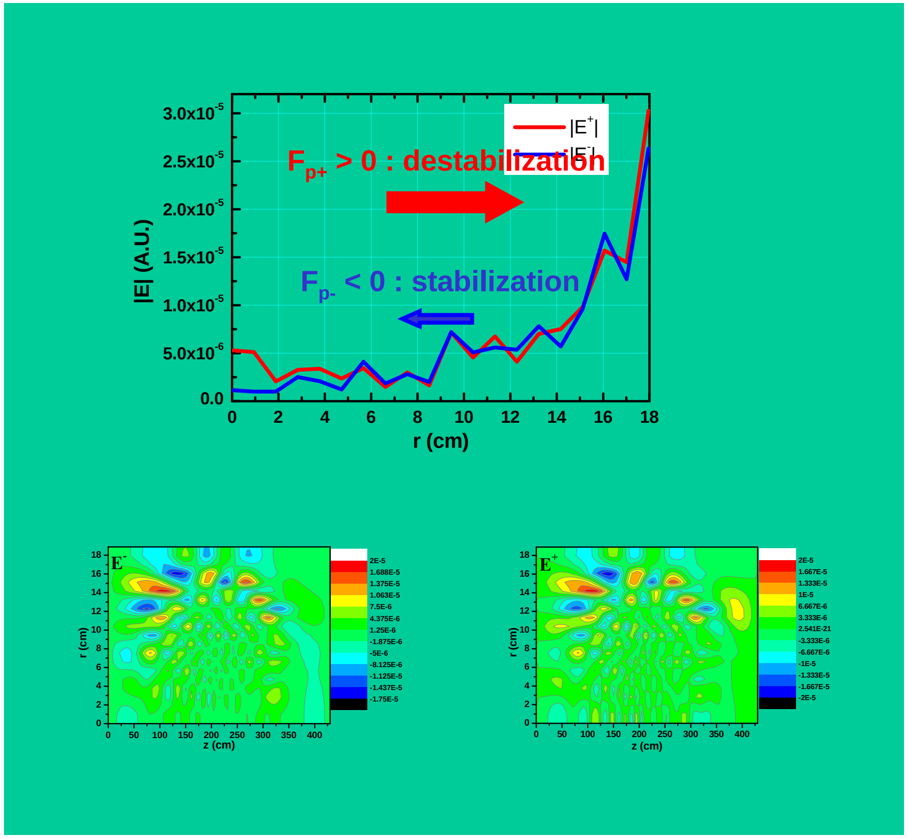

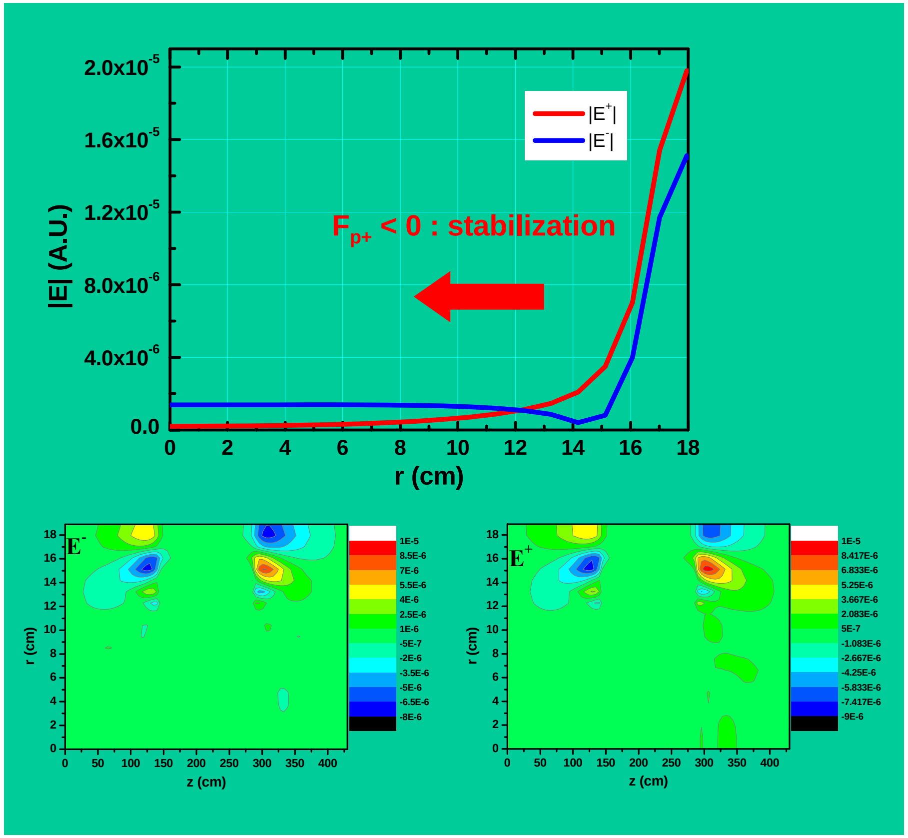

New Theory : EPM + SBC

Low-frequency electrostatic interchange mode

$$\frac{\partial n_{\omega\alpha}}{\partial t}+\nabla\cdot\mathbf{\Gamma}_{\omega\alpha}=0$$

Total ponderomotive force density

Collisional friction

Centrifugal force

$$m_\alpha\frac{\partial}{\partial t}\mathbf{\Gamma}_{\omega\alpha}+m_\alpha(\mathbf{V}_0\cdot\nabla)\mathbf{\Gamma}_{\omega\alpha}=q_\alpha\left[n_0\mathbf{E}_\omega+\frac{\mathbf{\Gamma}_{\omega\alpha}}{c}\times\mathbf{B}_0+\sum_{\omega'+\omega''=\omega}\left(n_{\omega'\alpha}\mathbf{E}_{\omega''}+\frac{\mathbf{\Gamma}_{\omega'\alpha}}{c}\times\mathbf{B}_{\omega''}\right)\right]+\nabla\cdot\Pi_{\omega\alpha}-m_\alpha\nu_\alpha\mathbf{\Gamma}_{\omega\alpha}+m_\alpha n_{\omega\alpha}\mathbf{g}_\alpha$$

Sideband waves

$$\frac{\partial n_{\omega_\pm\alpha}}{\partial t}+\nabla\cdot\mathbf{\Gamma}_{\omega_\pm\alpha}=0$$

Nonlinear coupling

$$m_\alpha\frac{\partial}{\partial t}\mathbf{\Gamma}_{\omega_\pm\alpha}=q_\alpha\left(n_0\mathbf{E}_{\omega_\pm}+\frac{\mathbf{\Gamma}_{\omega_\pm\alpha}}{c}\times\mathbf{B}_0+n^{\pm}_{\omega_s\alpha}\mathbf{E}_{\omega_0}\right)-m_\alpha\nu_\alpha\mathbf{\Gamma}_{\omega_\pm\alpha}$$

Plasma fluctuation driven by RF

$$\frac{\partial n_{\omega_0\alpha}}{\partial t}+\nabla\cdot\mathbf{\Gamma}_{\omega_0\alpha}=0$$

$$m_\alpha\frac{\partial}{\partial t}\mathbf{\Gamma}_{\omega_0\alpha}=q_\alpha\left(n_0\mathbf{E}_{\omega_0}+\frac{\mathbf{\Gamma}_{\omega_0\alpha}}{c}\times\mathbf{B}_0\right)-m_\alpha\nu_\alpha\mathbf{\Gamma}_{\omega_0\alpha}$$

+ Maxwell equations for RF and SB waves

- The stable operation window and its dependence on **RF-power** and ω_0/Ω_i agree well with experimental results.

Stable Operation Window: $0.95\le\frac{\omega_0}{\Omega_i}\le 1.02$

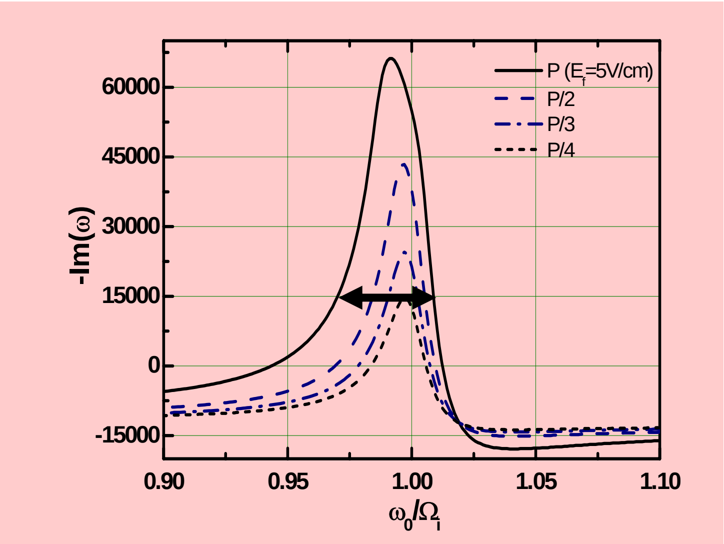

Idea for Improving Stability

- Hot electron ring formation
- Kinetic stabilizer
- Line–tying plate
- Divertor in central cell
- Cusp–baseball coil configuration
- RF stabilization (ponderomotive force)

Hot Electron Ring Formation

- D'Ippolito, et al. proposed the creation of hot-electron rings and disks in the end cells of a tandem mirror.
- The intent was to maximize the line bending of the mode.
- Maximizing the stabilizing mode line bending energy is equivalent to minimizing the parallel connection length between the central cell and the line-tying point.
- Theoretical arguments suggest that a high-β hot electron ring will support a higher central cell β for a ring beta, $\beta_r < 0.6$.
- But a high-β hot-electron disk should support a higher central cell beta for $\beta_r > 0.06$

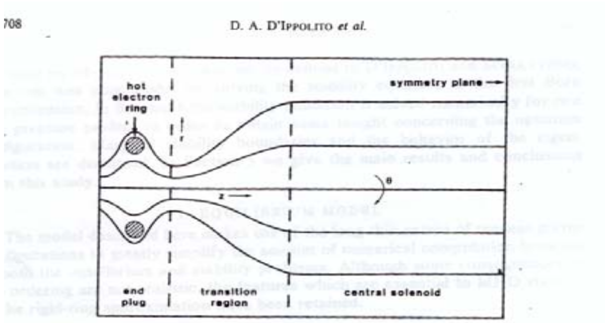

FIG. 1.—A sketch of the electron-ring-stabilized tandem mirror configuration discussed in the text showing a few typical field lines. The system is axisymmetric ($\partial/\partial\theta = 0$) and mirror symmetric about the midplane, so only the left half is shown.

There is little evidence that a high-β hot-electron disk has ever been made in a mirror machine

D. A. D'Ippolito,et al., Plasma Physics, ***24****, 707, (1982)*

RF Heating Studies

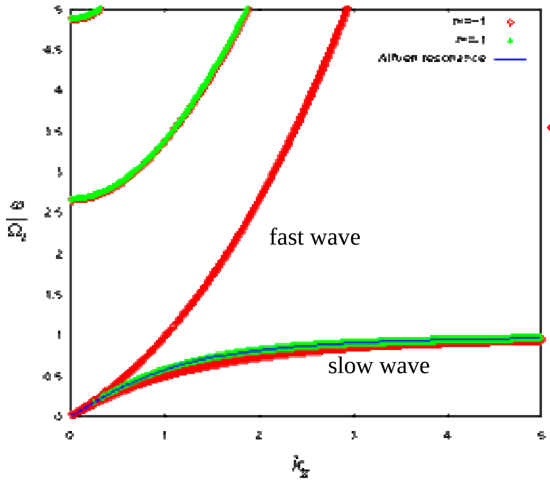

dispersion relation of magnetized cylindrical plasma

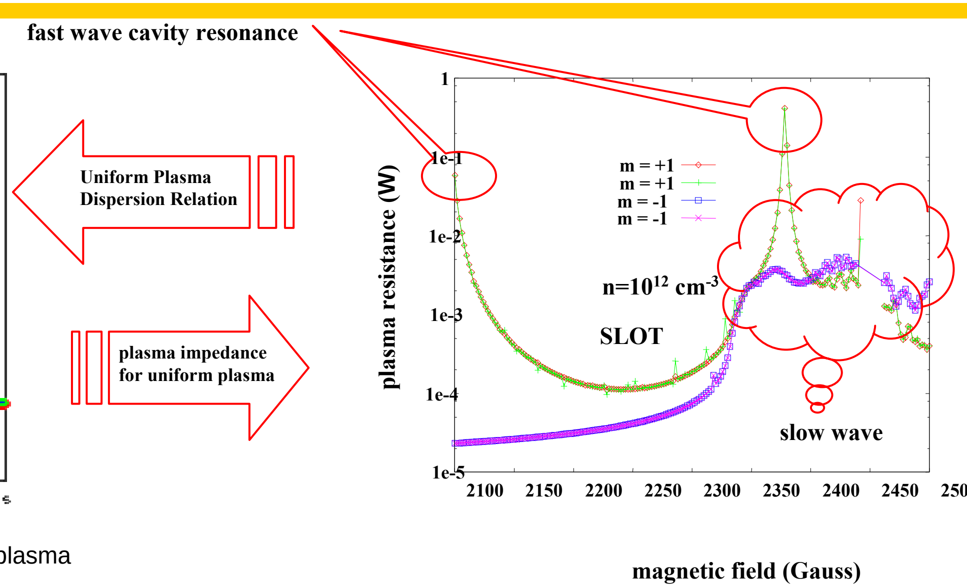

→ calculated by $\frac{1}{I_a^2}\int \vec{J}^* \cdot \vec{E} dr^3$ in the plasma volume.

→ calculated by $\oint \vec{S} \cdot \hat{n} da$ on the plasma vacuum boundary.

The plasma resistances calculated two ways are well coincident. This is necessary condition for exact solution.

- **The numerical results show that the RF wave can deliver its power to plasma more effectively as w/W$_{c0}$ < 1 for both of electron and ion *(left figure)*.**
- **The trend of power absorption into electron coincides very well with the trend of the plasma density *(right figure)*.**

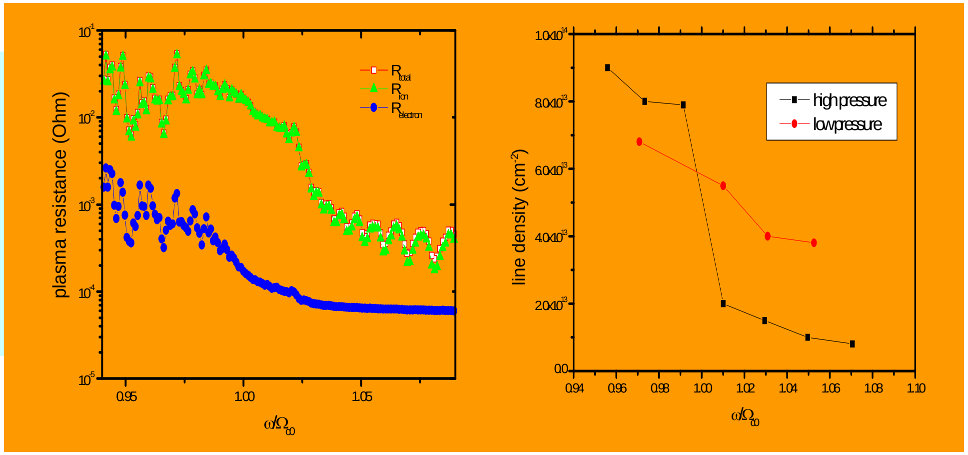

Application to HANBIT Mirror Device

representative wave patterns, m= +1, $Im(E_{r,\theta,z})$

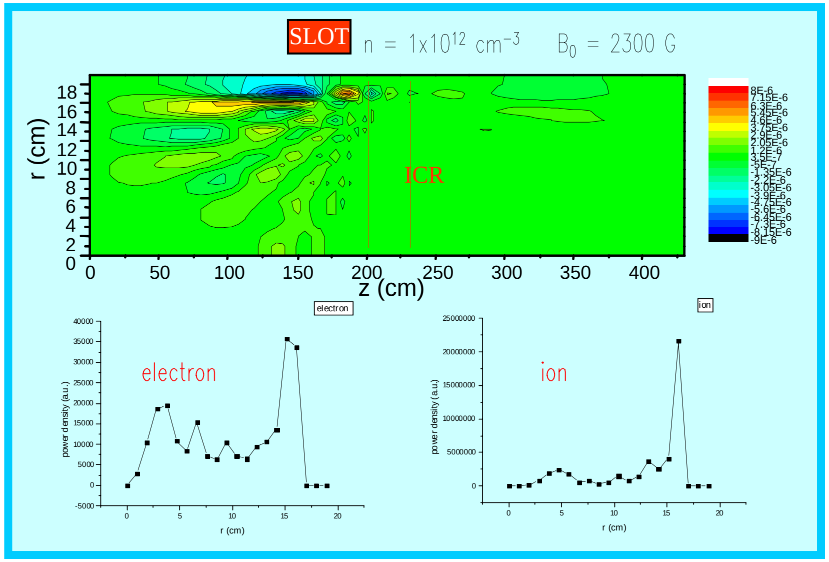

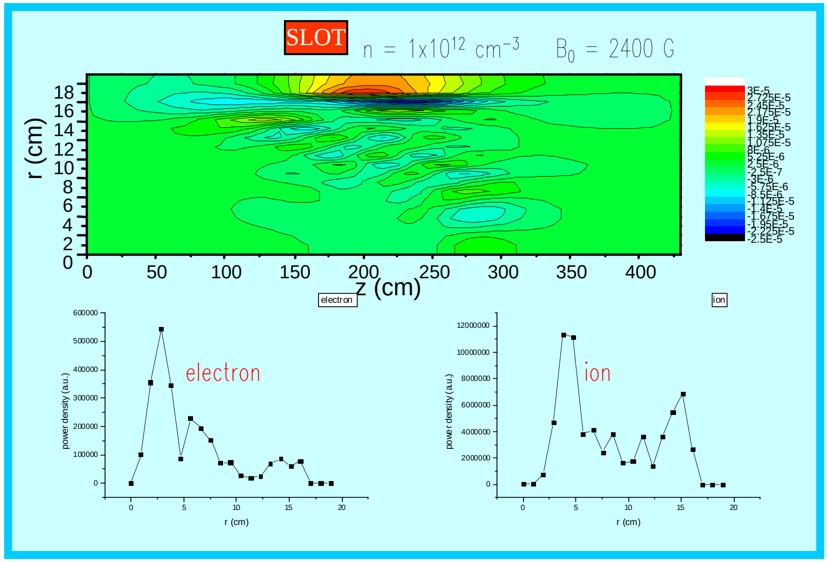

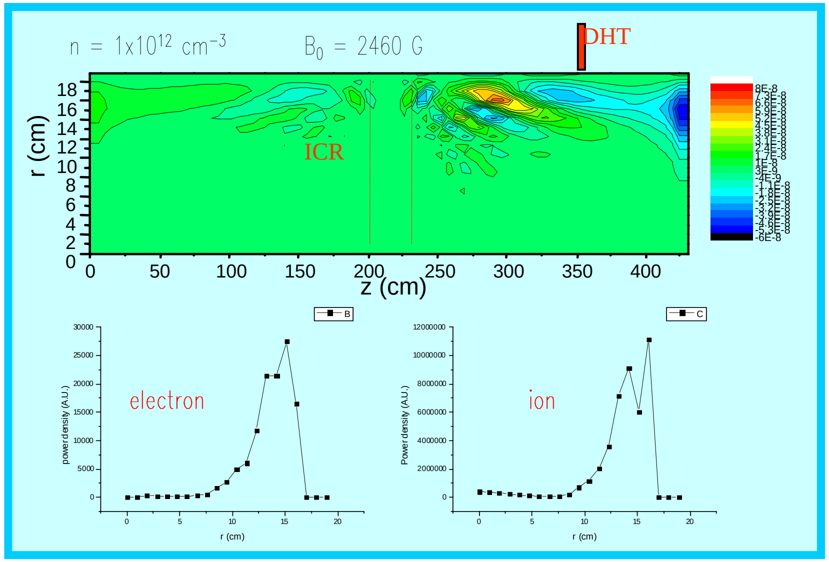

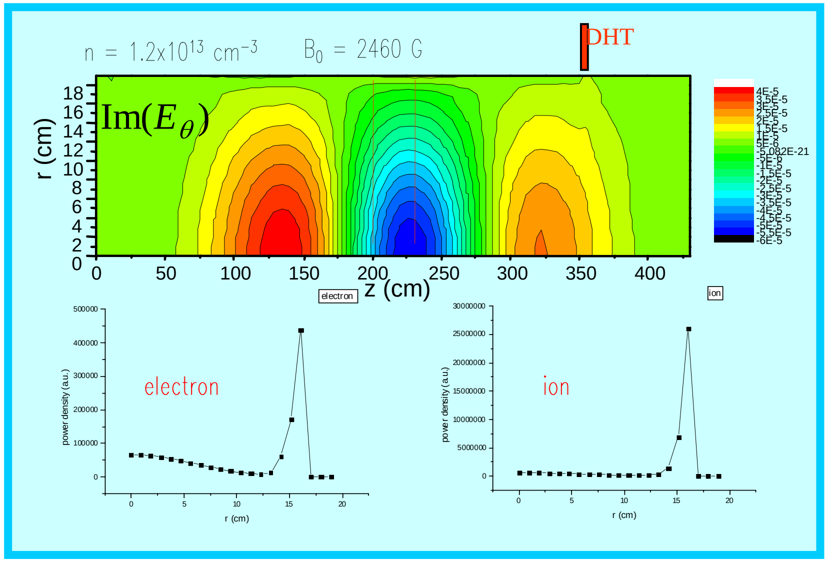

Effect of Neutral Pressure

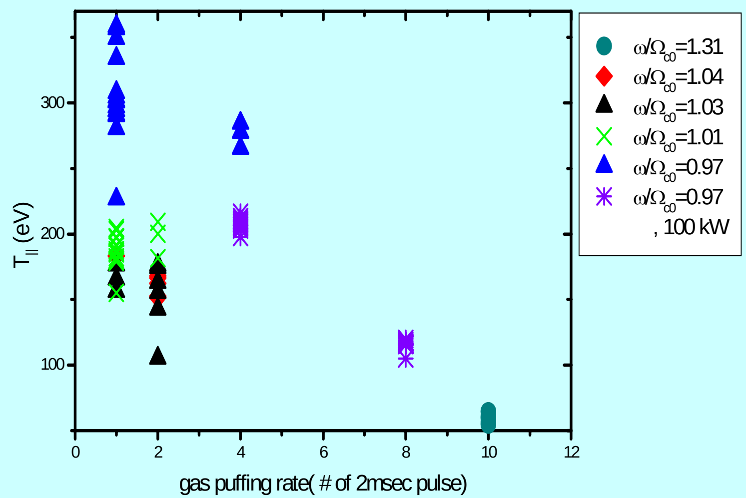

Low pressure discharge is effective to enhance the ion temperature.

Each point is time averaged $T_{||}$ for each shots to achieve representative value. It shows that temperature is increases as the reducing the number of puffing pulses.

RF: 150 kW
Puffing rate: 1 x pulse (2m sec)

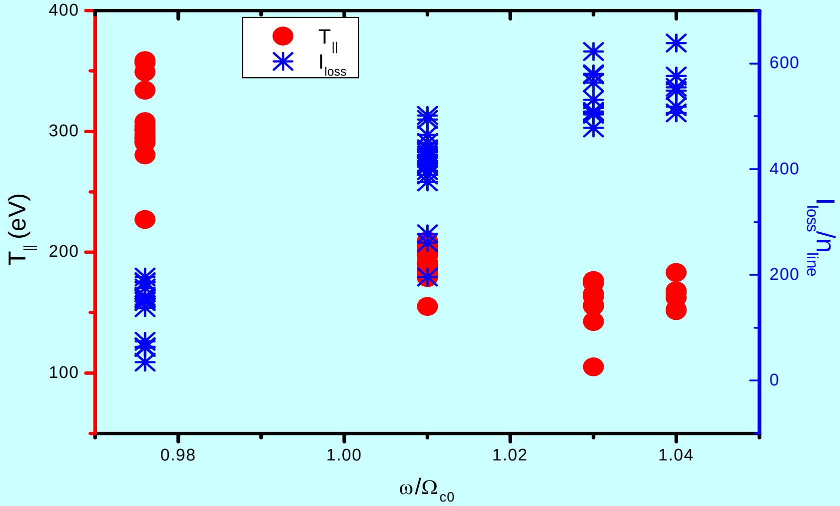

We performed time average for each shots again to achieve evident behavior of $T_{||}$ & I_{loss} on external magnetic field. We can see that at ω/Ω_{c0} < 1 case, parallel ion temperature is higher than ω/Ω_{c0} > 1 case and also temperature anisotropy becomes larger. It means that perpendicular temperature is much higher at ω/Ω_{c0} < 1 case.

New Operation Regime

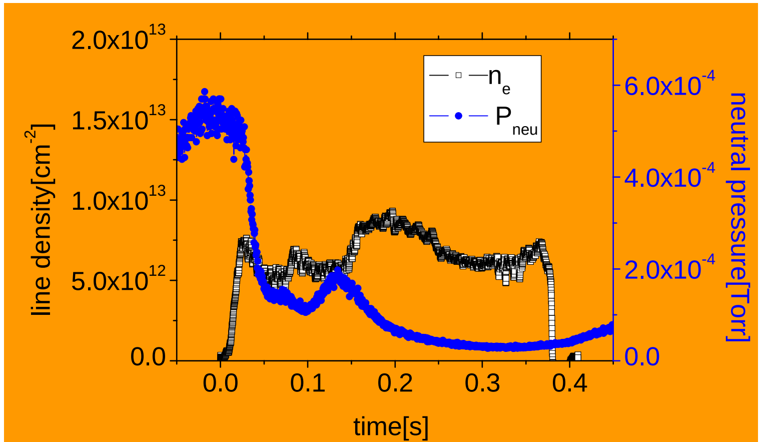

high gas pre-puff, 150kw rf

$$\omega / \omega_{ci} = 1.33$$

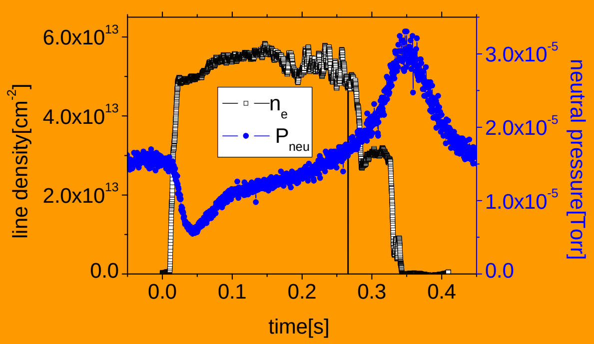

low gas pre-puff, 150kw rf

$$\omega / \omega_{ci} = 0.96$$

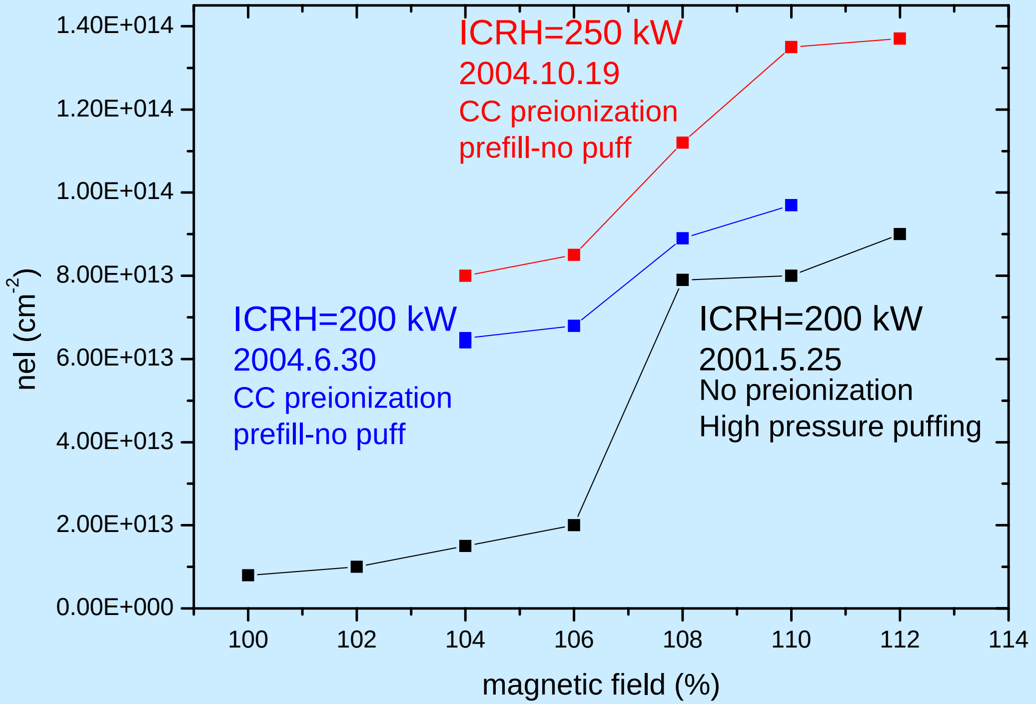

- Preionization with no puffing in central cell produces high density plasmas
- The usual transition to low density plasmas at low fields is not observed as low as 104%

Discharge Simulation-Radial Transport Model

Neutral continuity $$\frac{\partial N_k}{\partial t} + \frac{\partial \Gamma_k}{\partial r} = S_k - \nu_k^l N_k$$

Ion continuity $$\frac{\partial n_i}{\partial t} + \frac{\partial \Gamma_i}{\partial r} = s_i - \nu_i^l n_i$$

Quasi-neutrality $$n_e = \sum_i n_i \Leftarrow \sum_i \frac{n_i}{\tau_{ci}} = \frac{n_e}{\tau_{ce}}$$ ambipolarity

Drift-diffusion $$\Gamma_i = \frac{1}{m_i \nu_i^*}\left(eE - \frac{\partial T_i}{\partial r}\right) n_i - \frac{T_i}{m_i \nu_i^*}\frac{\partial n_i}{\partial r}, \qquad E = -\frac{\partial \phi}{\partial r}$$

Ion temperature $$\frac{\partial T_i}{\partial t} + \frac{\partial}{\partial r}(VT_i) - \frac{T_i}{3r}\frac{\partial}{\partial r}(rV) + \frac{2}{3n_e r}\frac{\partial}{\partial r}(rq_i)$$
$$= \frac{2P_{abs,i}}{3n_e} + \frac{(T_e - T_i)}{\tau_{ie}} - \frac{2}{3n_e}\sum_i\left(\varepsilon_i n_i N_i k_i^{ex} + E_{li}\frac{n_i}{\tau_{ci}}\right)$$

Electron temperature $$\frac{\partial T_e}{\partial t} + \frac{\partial}{\partial r}(VT_e) - \frac{T_e}{3r}\frac{\partial}{\partial r}(rV) + \frac{2}{3n_e r}\frac{\partial}{\partial r}(rq_e)$$
$$= \frac{2P_{abs,e}}{3n_e} + \frac{(T_i - T_e)}{\tau_{ie}} - \frac{2}{3n_e}\left(P_{inel} + E_{le}\frac{n_e}{\tau_{ce}}\right)$$

Heat flux $$q_i = -\frac{4.7 n_i T_i}{m_i \nu_i^*}\frac{\partial T_i}{\partial r}, \qquad q_e = -\frac{2 n_e T_e}{m_e \nu_e^*}\frac{\partial T_e}{\partial r}$$

Simulation results for plasma density and temperature at 1.6×10^{-5} Torr . Solid lines and circles represent simulation result and Langmuir probe measurement data, respectively. Square represents ion temperature estimated by semi-empirical method.

Plasma Density Profile

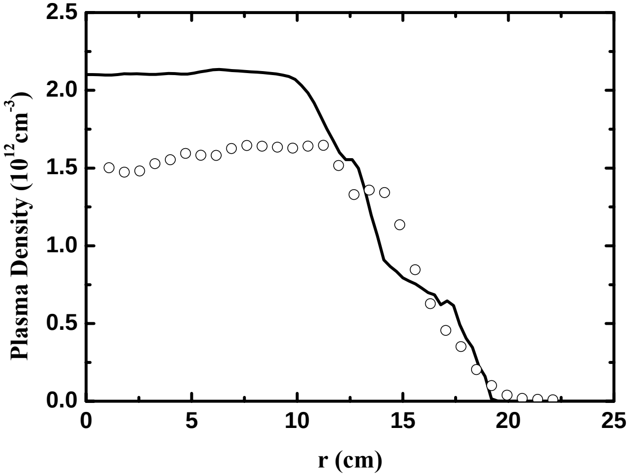

Temperature Profile

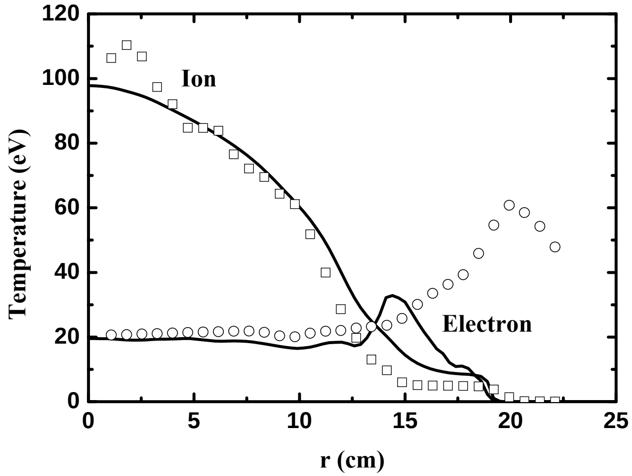

Simulation Results - DEGAS2

Calculated radial profiles

low gas puff, 150kw ICRH
$\omega / \omega_{ci} = 1.0$

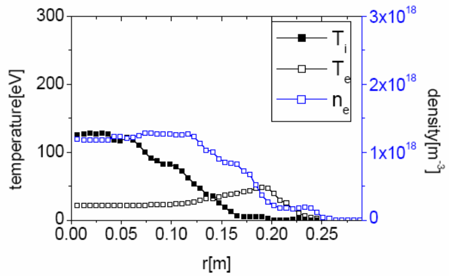

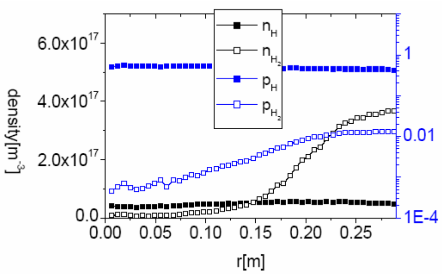

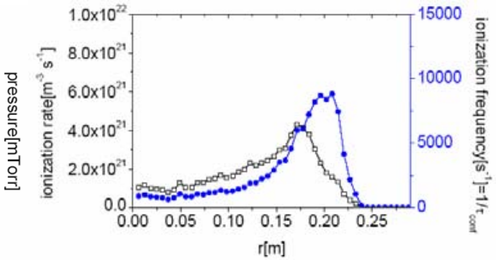

low gas puff, 150kw ICRH
$\omega / \omega_{ci} = 0.96$

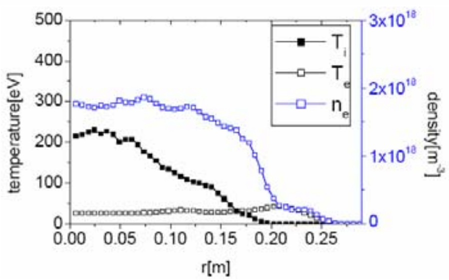

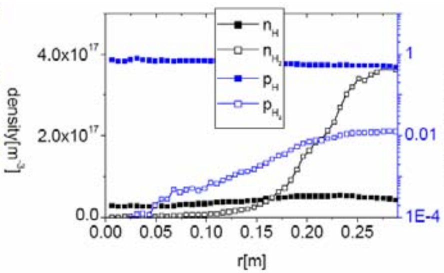

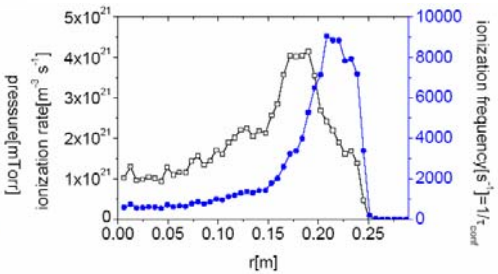

Loss power calculations

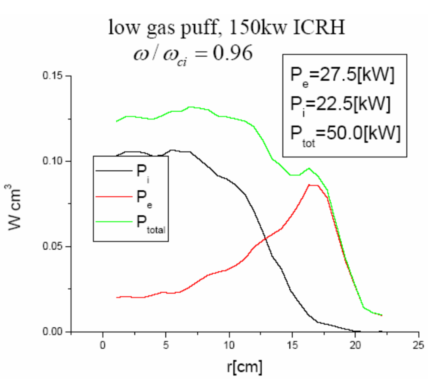

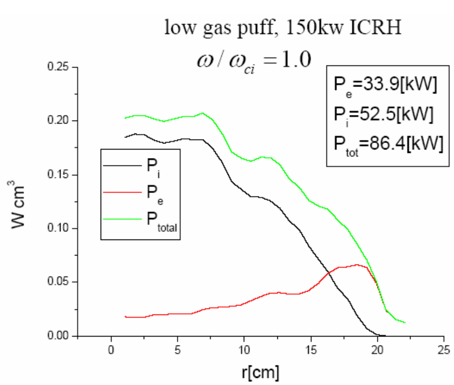

Particle balance and recycling coeff.

$$S_{puff} + S_{recycle} = L_{pump} \quad [m^{-3} s^{-1}]$$

	S_{puff} (max)	$S_{recycle}$	γ
$\omega / \omega_{ci} = 0.96$	3e17	8.7e20	1.58
$\omega / \omega_{ci} = 1.0$	3e17	6.7e20	1.41

Neutral hydrogen density

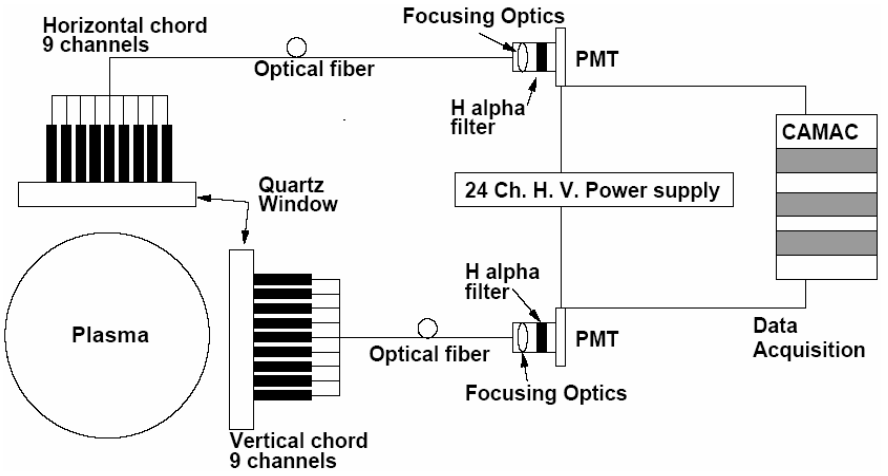

Emissivity profiles (#19937)

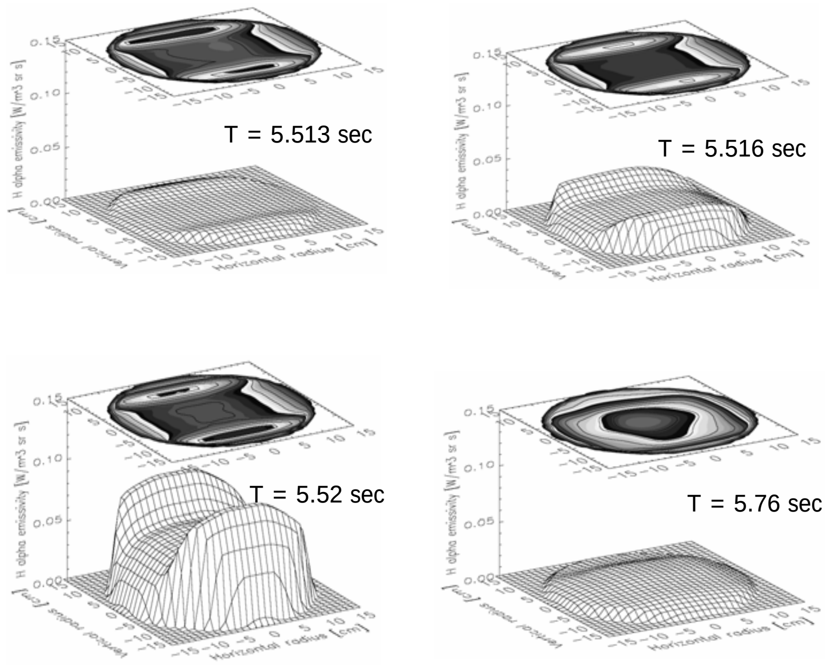

The reconstruction is performed for a square region of 32 cm x 32cm, which is divided into 30 x 30 equally spaced pixels about 1.1cm in length.

Bayesian Probability Theory (BPT) with MaxEnt method

Neutral hydrogen density profiles (#19937)

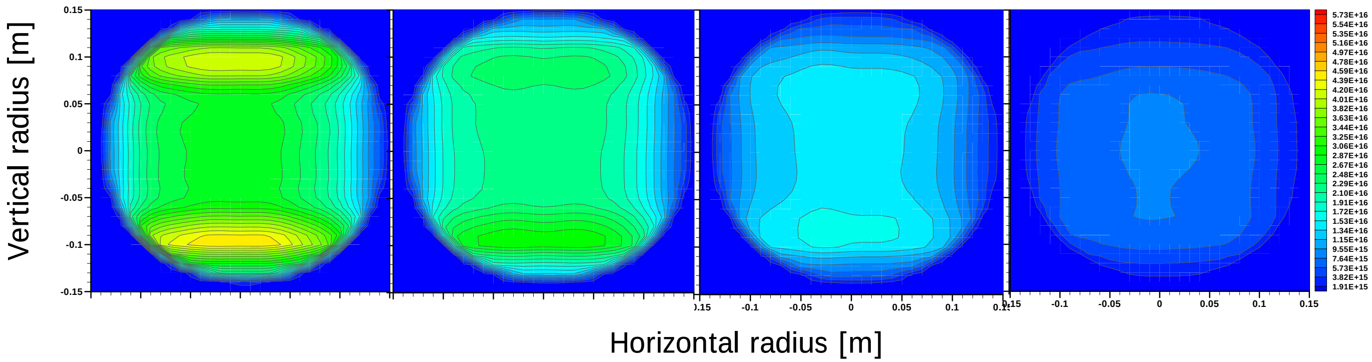

Summary

RF has significant effects on mirror MHD phenomena

Theories indicate that HANBIT experiments are in the range where sideband coupling effects are dominant over ponderomotive force effects.

Various methods for stabilization have been tried

A hot-electron ring has been created in the plug section of Hanbit. The β is not large enough to permit stabilization of the central cell plasma. The kinetic stabilizer is being under test. Other options are also being considered.

Low pressure helps increase temperature

Low pressure discharge is now available with pre-ionization. Order of magnitude reduction of the initial pressure reduces the charge exchange loss substantially.

Plasma modeling and neutral transport studies help characterize HANBIT plasmas

A heuristic plasma model based on Degas2 and 1-D plasma transport is developed and it reproduces the experimental plasma quite reliably.
(accurate measurement of Te and ne profiles are essential)

For ion heated plasma, Ti is limited mainly by high wall recycling rate due to excessive charge-exchange process